Magnetism and Superconductivity Sharing a Common Border in Organic Conductors

D. Jérome

Laboratoire de Physique des Solides,

Université Paris-Sud, 91405, Orsay, France

Abstract

The class of organic solids based on cation radical salts deriving from the parent molecule TTF provides one- and two-dimensional conductors (superconductors) in which the electron delocalization proceeds via a strong overlap between neighbouring molecules. Their magnetic properties reveal in both series a common border between magnetism and superconductivity. Furthermore, the existence of antiferromagnetic fluctuations in the conducting phase is clearly established by susceptibility and NMR experiments. Magnetism is also relevant in the alkali-doped fullerene A_1C_{60} and gives rise to an antiferromagnetic ground state and strong ferromagnetic fluctuations at high temperature.

1 Introduction

The development of itinerant magnetism in organic conductors is tightly linked to the history of organic superconductivity. Magnetism is indeed found in the same materials, where conductivity and superconductivity can be stabilized at low temperature, although under different conditions. The actual start of the research on organic conductors was 1972 when a metallic-like conduction and a huge increase of conductivity down to 60 K was reported in the organic charge compound TTF-TCNQ before a Peierls transition (Jérome and Schulz, 1982). In this material, conduction proceeds very much like in a regular metal although no metal atoms are present in the molecules. This is the characteristics for organic conductivity. Soon after the discovery of organic superconductivity, itinerant magnetism appeared to be a frequently accompanying phenomenon. Contrasting with conventional molecular crystals made of neutral organic molecules held together by weak Van der Waals forces, organic conductors contain molecules with unpaired carriers in π-molecular orbitals presenting an open shell configuration. Such a situation originates from a partial oxidation (reduction) of donor (acceptor) molecules in the formation of a salt with an inorganic anion (cation). In addition, a strong inter-

molecular overlap of π-orbitals allows the electron delocalization over all molecular sites in the crystal. However, in most cases the delocalization occurs preferentially along selected crystallographic directions. Such a packing optimizes the overlap

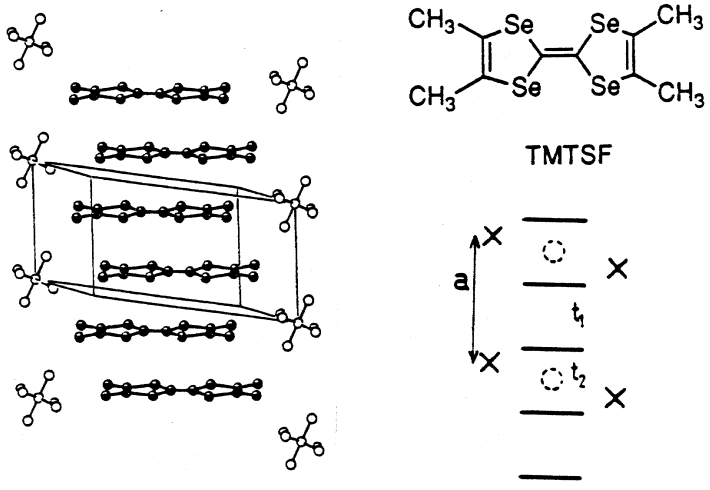

Figure 1. Donor molecule TMTSF, entering the Q-1D structure of $(TM)_2X$ compounds. The structure is dimerized with an alternating intermolecular distance (overlap integrals).

between molecular orbitals along the stacking direction. As long as the on-site Coulomb repulsion U does not overcome the energy gained by the band formation, conducting properties can be observed with a very pronounced one dimensional character along the stacking axis. The planar TMTSF (tetramethyl-tetraselena fulvalene) donor molecule with the TTF skeleton forms loosely connected stacks of molecules in the crystalline state of $(TMTSF)_2X$ salts (Fig. 1, where the organic molecule is oxidized in the presence of an inorganic acceptor X = PF_6, ClO_4, NO_3,...) (Bechgaard et al., 1980).

Other derivatives of the TTF molecule also give rise to higher dimensionality conductors. These are the planar donor molecules BEDT-TTF (ET) (Williams et al., 1991). The κ-type packing of ET molecules is unique in that the molecules first form dimers and then adjacent dimers are arranged in planes in an almost orthogonal order (Urayama et al., 1988), Fig. 2. Intra and interdimer interactions are nearly equal in amplitude. Secondly, the planes are packed in a 3D structure

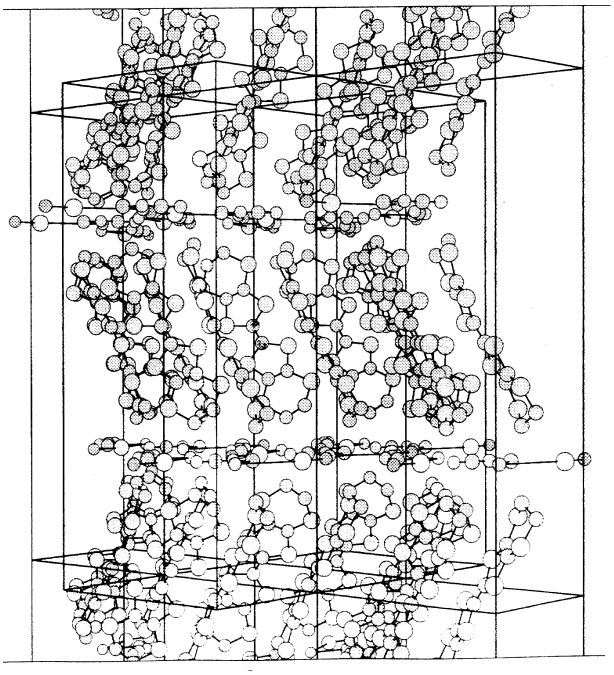

Figure 2. Transverse view of the 2D organic superconductor κ-$(ET)_2Cu[N(CN)_2]Br$.

of $(ET)_2X$ materials with an alternation of organic and inorganic planes of anions $X = Cu(NCS)_2$, $Cu[N(CN)_2]Br$ (or Cl), etc. . . .

This crystal structure gives rise to a large metal-like conduction within the molecular layers and a very loose coupling between layers. In both 1- and 2D series, the negatively charged anions adopt a closed-shell configuration and do not contribute to the electrical conduction. So far, we have introduced organic compounds displaying 1- or 2D conducting properties. However, the recent discovery of the C_{60} molecule (Kroto et al., 1985) has allowed the synthesis of isotropically conducting organic solids. Unlike the TMTSF molecule (called TM from now on), neutral C_{60} molecule is a good electron acceptor molecule. Hence, when electrons are added to the LUMO of individual molecules through their reduction by an alkali cation the strong intermolecular interaction between π-orbitals makes a salt such as A_3C_{60}, A = K, Rb, Cs a 3D conductor and even a superconductor (Hebbard et al., 1985), Fig. 3. We shall restrict the subject of this review to the three families of organic conductors which have been mentioned above. They all exhibit superconductivity

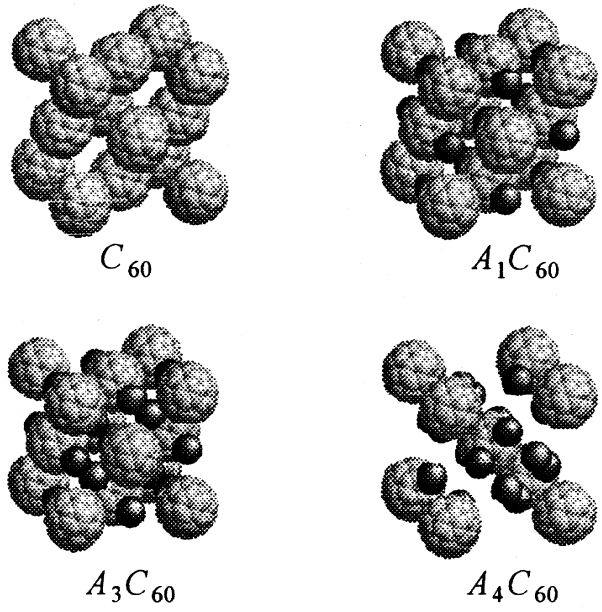

Figure 3. Crystal structures of C_{60} and various alkali-doped fullerides, after Goze (1996).

with critical temperatures ranging between 1 and 30 K in the 1-, 2- and 3D series. They can also exhibit itinerant antiferromagnetic ground states instead of superconductivity and strong magnetic fluctuations at high temperature. A conduction band formed by the intermolecular overlap of π-molecular orbitals giving rise to bandwidths of the order of 1 eV, Fig. 4.

The family of organic conductors extends far beyond those discussed in this short survey but the interplay between magnetism and superconductivity is best illustrated by the restricted choice made in this article.

2 One dimensional conductors

2.1 Materials

Practically all properties that can be anticipated from the theory of 1D conductors (Solyom, 1979) are observed in the prototypic family $(TM)_2X$ where TM means the symmetrical TMTSF molecule or its sulfur analogue TMTTF and X is a monoanion such as an halogen or PF_6, ClO_4, etc$\cdots$. This brief review will not discuss

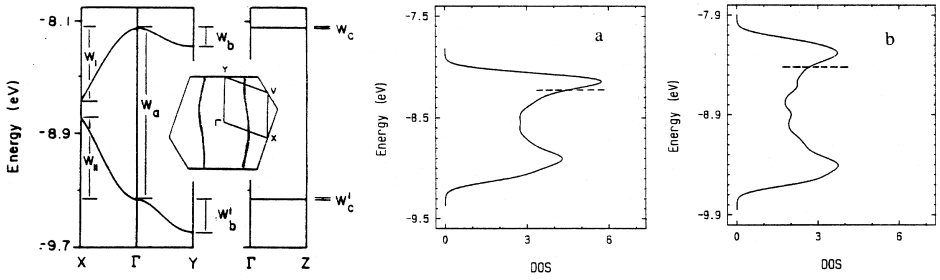

Figure 4. Energy dispersion of $(TMTSF)_2PF_6$ using the double ζ calculation and density of states or $(TMTTF)_2Br$ (a) and $(TMTSF)_2PF_6$ (b) (E. Canadell, 1995). The interchain coupling is responsible for the small warping of the Fermi surface. The dimerization gap is visible at the point X of the zone boundary. The minimum near the center the density of states is a reminiscence of the dimerization.

the properties related to structural disorder introduced by non symmetrical molecules such as TMDTDSF (Auban, 1989), DMET (Ishiguro and Yamaji, 1990), or by alloying the organic stack. According to the 2 : 1 stoichiometry of the salt, oxidation of the neutral TM molecule should lead to the presence of half a hole per TM molecule. However, the intermolecular distance along the stacking direction in the crystal exhibits a dimerization with the important consequence of opening a dimerization gap in the 1D electron dispersion (Ducasse et al., 1986), hence, the 1D conduction band becomes half-filled instead of 3/4-filled as can be inferred from chemical considerations only. The conduction band is about 1 and 0.5 eV wide for TMTSF and TMTTF salts respectively, Fig. 4. It will become clear that the half-filling character is one of the crucial parameters which governs the electronic properties of these materials at low temperature. This property can be related to the gap δ_G (the dimerization gap) which is opened in the middle of the originally 3/4 filled band and gives rise to full (empty) lower (upper) bands. The dimerization gap is related to the alternation of the intra stack transfer integral. Structure determinations and band calculations show that the relative bond alternation is large for sulfur based molecules 38% in $(TMTTF)_2PF_6$ and smaller in selenium compounds 19% and 15% in $(TMTSF)_2PF_6$ and $(TMTSF)_2ClO_4$ respectively with a further decrease under pressure and (or) at low temperature due to thermal contraction. There exists a finite (although small) interstack coupling $t_\perp$ which makes these 1D conductors actually quasi-1D (Q-1D) when the temperature is smaller than a cross-over temperature T_x. In a non-interacting electron gas T_x reads $T_x^0 = t_\perp/\pi$ (Emery, 1983). However the cross-over temperature is influenced by Coulombic intrachain interactions and T_x could very well be much smaller than the bare cross-over temperature T_x^0 (vide-infra). Consequently, we may anticipate that sulfur compounds in the $(TM)_2X$ series with large dimeriza-

tion gaps and low cross-over temperatures should exhibit more pronounced 1D features than the selenium-based conductors. Such an expectation is corroborated by the examination of the $(TM)_2X$ phase diagram.

2.2 High temperature regime

Electronic, magnetic and structural properties of $(TM)_2X$ compounds are now fairly well understood in a quasi-one dimensional (Q-1D) theoretical framework where the band-filling character, the amplitude of the Coulomb repulsion and intra (inter) chain overlaps are the relevant parameters. The generic diagram in Fig. 5 displays the variety of regimes than can be observed among $(TM)_2X$ compounds (Jérome, 1991). Special attention has been paid to key compounds on which transport, magnetic, NMR and structural experiments have been performed varying the temperature or pressure. They are labeled by letters in Fig. 5. The transport in the high temperature domain ($T \geq 300$ K) is governed by the strength of the 1D lattice dimerization. This dimerization makes the half-filling of the band a particularly relevant concept for compounds at the left of the diagram but much less pertinent (although non zero) where moving towards the right. The band structure of these 1D conductors is relatively simple as it comprises two nearly planar and open Fermi surfaces, Fig. 4. The interactions between electrons are usually taken as three constants g_1, g_2 and g_3 modeling the backward, forward and Umklapp scattering of two electrons respectively. When the band is half-filled, the scattering of two electron from one side of the Fermi surface to the other via the Umklapp repulsion $g_3 = g_1 \frac{\delta_G}{E_F}$ contributes to localize the 1D carriers (Barisič and Brazovskii, 1979) since the momentum transfer in this scattering is a reciprocal lattice vector. The transport becomes activated below a temperature with an activation energy $\Delta_\rho = \pi T_\rho$ (Emery et al., 1982). $(TMTTF)_2PF_6$ (a) provides a good example for the strong Mott-Hubbard localization $\Delta_\rho \approx 600$ K of carriers in a half-filled band. The magnetism of such a Mott-Hubbard localized phase is that of a 1D Heisenberg chain. The uniform susceptibility ($q = 0$ fluctuation modes) follows a Bonner-Fisher behaviour with a maximum at a temperature inversely proportional to Δ_ρ. The $2k_F$ fluctuations modes are also low lying excitation mode of this AF chain. They can be probed by the measurement of the hyperfine spin-lattice relaxation rate T_1^{-1} (Moriya, 1963) which reads for a 1D conductors (Bourbonnais, 1987),

$$T_1^{-1} = C_0 T \chi_S^2(T) + C_1 T^{K_\rho} \tag{1}$$

where $q = 0$ ($2k_F$) spin fluctuations contribute to the first (second) term in Eq. (1). K_ρ is the exponent related to the spatial dependence of the charge-charge correlation function in 1D theory (Schulz, 1991). It also enters the power law temperature dependence of the density wave (DW) response at $2k_F$, namely

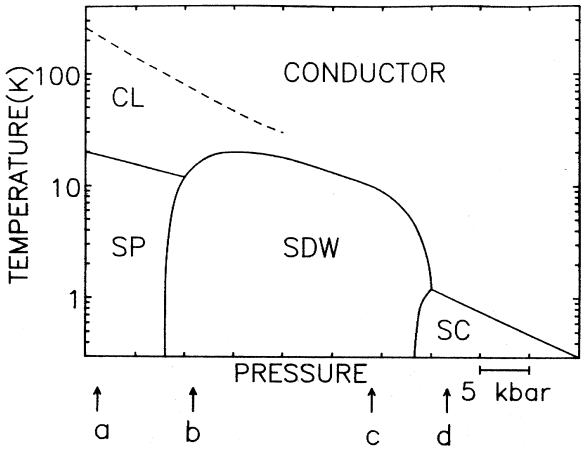

Figure 5. Generalized phase diagram for the $(TM)_2X$ series. Spin-Peierls (SP), spin density wave (SDW) and superconductivity (SC) are indicated together with the zero pressure location of prototypical compounds $(TMTTF)_2PF_6$ (a), $(TMTTF)_2Br$ (b), $(TMTSF)_2PF_6$ (c) and $(TMTSF)_2ClO_4$ (d). The dotted line represents the temperature T_ρ separating the metallic phase at high temperature from the charge localized phase (CL) at low temperature.

$\chi_{\rm DW}(2k_F) \approx T^{K_\rho - 1}$. If 1D charge localization comes into play, $K_\rho \to 0$, and the $2k_F$ contribution to T_1^{-1} should become T-independent according to Eq. (1).

The temperature dependence of T_1^{-1} of $(TM)_2X$ compounds provides a remarkable illustration for the evolution between Mott-Hubbard localized electrons in (a) and delocalized 1D electrons in selenium compounds (c) and (d), Fig. 6. In those selenium compounds, because of the weakness of the half-filling character, 1D Mott-Hubbard (localization is not efficient until a cross-over towards a 2- or 3D electron gas is reached at the cross-over temperature T_x). It has been pointed out that the cross-over temperature can be strongly suppressed by intrachain Coulombic interaction in the Q-1D electron gas and should read (Bourbonnais and Caron, 1986)

$$T_x = T_x^0 \left(\frac{t_\perp}{E_F} \right)^{\frac{1-K_\rho}{K_\rho}} \tag{2}$$

According to Eq. (2), a single particle cross-over temperature is either non relevant or at most very small whenever the Mott-Hubbard localization is developed. This is the situation which is encountered for sulfur compounds with $K_\rho \to 0$. For selenium compounds, Umklapp can no longer be a strong localizing mechanism although strong $2k_F$ fluctuations are still seen by NMR experiments and a metal-

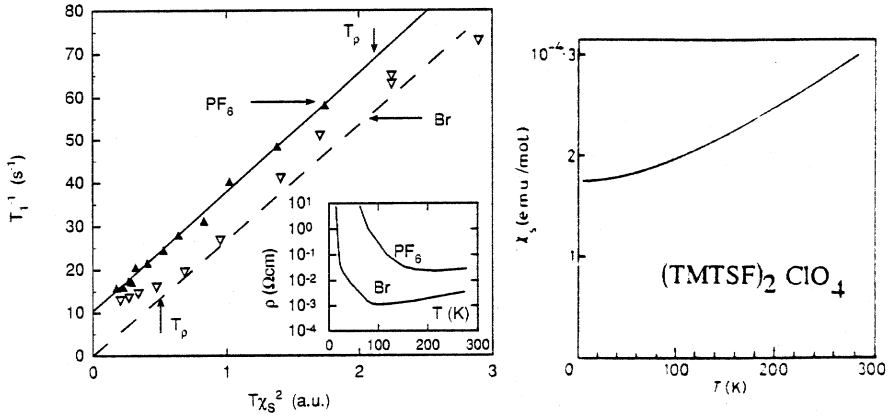

Figure 6. ^{13}C-relaxation rate of two compounds of $(TMTTF)_2X$ series versus $T\chi_S^2$, X = PF_6 and Br. T_ρ is the temperature showing the charge localization. The localized limit is reached at low temperature in all sulfur compounds. The finite intercept of T_1^{-1} at $T = 0$ is attributed to the role of 1D AF-fluctuations. These fluctuations, although present in selenium compounds as well cannot be detected on such a plot, see the dashed line for the schematic behaviour of $(TM)_2X$ compounds. The T-dependence of the spin susceptibility is similar throughout the $(TM)_2X$ series.

like behaviour survives down to a critical temperature where the conducting state undergoes a transition towards an itinerant magnetic ground state (Bechgaard et al., 1980; Jérome and Schulz, 1982). The extensive NMR investigation conducted in various compounds of the $(TM)_2X$ series (Wzietek, 1993) has led to a determination of the intrachain interactions governing the magnetic and transport properties of the 1D metallic phases (Jérome, 1994).

Table I: Parameters describing the behaviour of transport (K_ρ, g_3) and magnetic properties (g_1) of some $(TM)_2X$ compounds in the conducting (or localized) phase at high temperature.

Compounds	T_ρ	K_ρ	$\frac{g_1}{\pi v_F}$	$\frac{g_3}{\pi v_F}$	T_x	E_F
$(TMTTF)_2PF_6$	> 250 K	0 ($T < 250$ K)	1	0.4	< 20 K	1600 K
$(TMTTF)_2Br$	100 K	0 ($T < 50$ K)	0.9	0.35	< 20 K	1900 K
$(TMTSF)_2PF_6$	No	0.15 ($T < 100$ K)	1.1	0.16	10 K	3100 K

2.3 $(TM)_2X$ ground states

At the left side of the diagram Fig. 5(a) $(TMTTF)_2PF_6$ presents an insulating spin-Peierls ground state in which the electrons of a uniform Heisenberg chain at high temperature are dimerized and form a non-magnetic singlet ground state with a $2k_F$-lattice distortion below $T_{SP} = 19$ K (Pouget et al., 1982). The spin-Peierls instability is slightly depressed under pressure (Jérome, 1991) and above 10 kbar a ground state with an internal magnetization is stabilized; a spin-density wave (SDW) phase with a commensurate wave vector (Brown et al., 1997). That is also the situation encountered in $(TMTTF)_2Br$ at ambient pressure (a) (Barthel et al., 1993). Increasing pressure, the Néel temperature increases and the commensurate antiferromagnetic Néel state becomes incommensurate above a critical pressure of 10 and 5 kbar for (a) and (b) respectively with a concomitant maximum of the AF transition temperature (Klemme et al., 1995), Fig. 7. The 3D coupling which promotes the existence of long-range order at low temperature is the intrachain interaction between $2k_F$ bond CDW for the spin-Peierls ground state and the interchain exchange coupling for the commensurate Néel instability (Bourbonnais, 1987). When the conducting phase is stable below T_x, it is the nesting properties of the 2D Fermi surface which triggers the establishment of the Overhauser ground state at T_N given by $1 - g_1(T_x)\chi_{SDW}(\mathbf{Q}, T) = 0$ where $g_1(T_x)$ stands for the amplitude of the electron interaction renormalized down to T_x and $\mathbf{Q}$ is the best nesting vector of the 3D Fermi surface (Ishiguro and Yamaji, 1990). With a 2D model for the Fermi surface (FS), $\mathbf{Q} = (2k_F, \pi/b)$ when only nearest neighbour interchain interactions are included in the energy dispersion, namely

$$\varepsilon(k) = 2t_{\|} \cos k_{\|} a + 2t_{\perp} cos k_{\perp} b. \tag{3}$$

Deviations to perfect nesting are taken into account by adding a contribution $2t'_{\perp} \cos 2k_{\perp} b$ to Eq. (3). Thus, the nesting vector becomes incommensurate with the underlying lattice. This is the situation which prevails in $(TMTSF)_2PF_6$ (c) at ambient pressure or in $(TMTTF)_2PF_6$ and $(TMTTF)_2Br$ under high pressure. Evidences for the incommensurability of the magnetic modulation have been given by NMR and transport properties experiments. The ^{13}C-NMR single crystal lineshape of $(TMTSF)_2PF_6$ reveals a continuous distribution of local fields (Barthel et al., 1993) instead of the narrow lines related to the finite number of magnetically inequivalent nuclei at high temperature.

At first sight, the field distribution can be explained by a sinusoidal modulation with amplitude (0.06–0.08 μ_B). This spectrum is at variance with the discrete NMR spectrum observed in the commensurate SDW of $(TMTTF)_2Br$ at ambient pressure using ^{13}C and ^{1}H-NMR.

Other evidences for the incommensurability of the SDW ground state are given

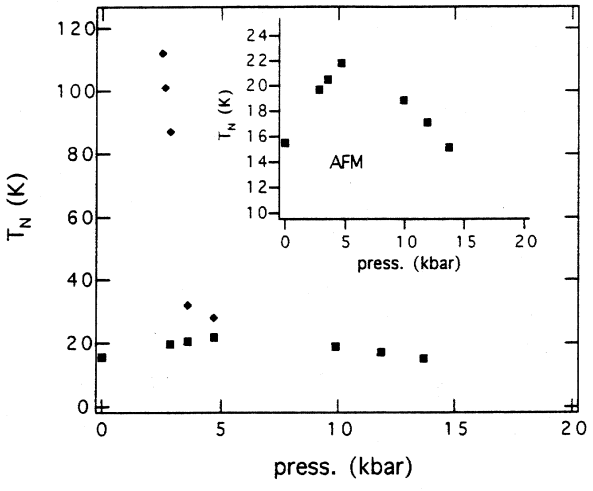

Figure 7. The SDW ground state of $(TMTTF)_2Br$ under pressure. 5 kbar is a critical pressure between a commensurate SDW ($P < 5$ kbar) and an incommensurate SDW at $P > 5$ kbar.

by the consequence of the existence of a low lying long wavelength phason mode in the excitation spectrum corresponding to the sliding of the modulation. This mode gives rise to a hyperfine relaxation of the nuclear spins which is T-independent when the SDW effective mass is not enhanced by a coupling to phonons (Barthel, 1994). This behaviour has been clearly identified in the SDW state of $(TMTSF)_2PF_6$ (Barthel et al., 1993a) and also in $(TMTTF)_2Br$ under 12 kbar (Klemme et al., 1996), Fig. 8. The behaviour of $(TMTTF)_2Br$ at 1 bar or $(TMTTF)_2PF_6$ at 10 kbar is in striking contrast. There, the gapless phason mode is suppressed by commensurability and nuclear relaxation is induced by the thermal excitation of magnon modes with an activation energy of ≈ 12 K at $H = 9.4$ T.

Another consequence of the SDW incommensurability can be observed in the transport properties of the Overhauser state. The magnetic incommensurate structure has no preferential position with respect to the lattice; it can slide and contribute to a collective conducting channel similar to the Fröhlich mode of CDW systems (Grüner, 1994). This mode consists in the joint displacement of both spin polarized CDW modulations building up the SDW ground state. Hence, the conductivity of the SDW state becomes electric field dependent. However, a non linear conductor is only observed above a threshold field E_T (of the order of 5 mV/cm (Tomič and Jérome, 1989)). The threshold field is related to the breaking of the translational invariance of the SDW by the existence of randomly distributed im-

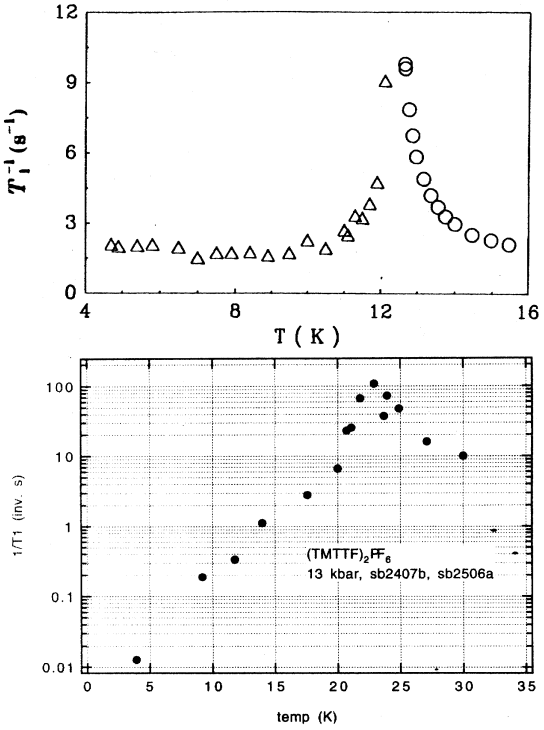

Figure 8. Temperature dependence of the ^{13}C-relaxation in the incommensurate SDW phase of $(TMTSF)_2PF_6$. The T-independent relaxation below the peak due to 3D fluctuations at T_N is attributed to the gap less phason mode. The relaxation is activated in $(TMTTF)_2PF_6$ under 13 kbar as the ground state is expected to be a commensurate SDW.

purities acting as pinning centers on the condensate, Fig. 9. The oscillation of the SDW condensate around its equilibrium position can contribute to the AC conductivity (at $E < E_T$) and gives rise to a resonance in the far infrared regime. This is the pinned mode resonance. The very large electrical polarizability of the condensate gives rise to a large static dielectric constant which in turn is related to the threshold field by the equation

$$\varepsilon(0)E_T = \text{constant}. \tag{4}$$

The validity of Eq. (4) has been proven for a variety of CDW phases (Grüner, 1988). It is also followed over a wide domain of threshold fields in the $(TMTSF)_2[AsF_6]_{(1-x)}[SbF_6]_x$ series as E_T is varied by several orders of magni-

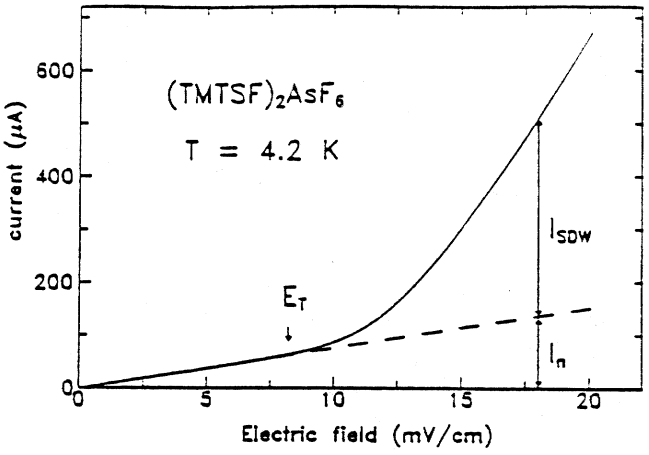

Figure 9. Non linear conduction in the SDW phase of $(TMTTF)_2AsF_6$ at $T = 4.2$ K.

tudes throughout the solid solution (Traetteberg et al., 1994). The DC collective motion of the SDW condensate generates an AC component at a frequency ν_n which is linearly related to the collective current. The existence of the oscillating current is well established in $(TMTSF)_2PF_6$ by looking at the interference between an external AC driging source and the internal AC current (Kriza et al., 1991). This is the equivalent of the Shapiro steps in the physics of Josephson junctions. Furthermore, the rigid motion of the magnetic modulation induces a local magnetic field modulation at a frequency ν_ϕ as observed from the magnetic motional narrowing of the NMR lineshape (Barthel et al., 1993b). There still remains a controversy about the relation between ν_n and ν_ϕ (at a given SDW current) in a SDW state. The origin of the AC current oscillation, rigid motion of the condensate or single particle to collective conversion at the electrodes is not settled for a SDW state (Clark, 1996).

A recent claim has been made about the existence of CDW x-ray scattering satellites (extremely weak) in the $(TMTSF)_2PF_6$ ground state at a wave vector $\mathbf{Q}$ corresponding to the wave-vector of the magnetic modulation (Pouget, 1996). The coexistence between magnetic and electric modulations implies that the two spin polarized CDW building up the SDW modulation are not exactly out of phase, as expected for a pure SDW. This mixture between degrees of freedom could possibly explain the weakly first-order character of the transition revealed in transport and magnetic measurements. The 2D nesting becomes frustrated when $2t'_\perp$ is increased (changing the anion or under pressure). Consequently the SDW ground state is rapidly suppressed. The possible divergence of the Cooper channel at low temper-

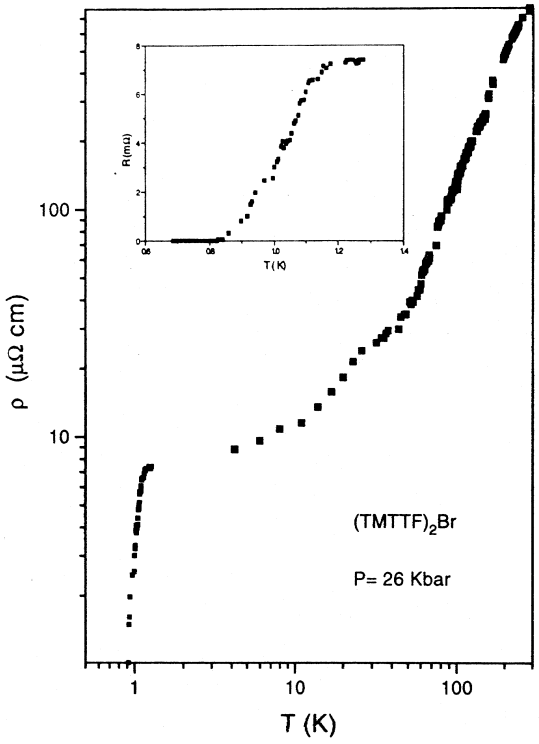

Figure 10. Superconducting transition in $(TMTTF)_2Br$ under 26 kbar.

ature is unaffected by the increase of $2t'_\perp$ since inversion symmetry $\epsilon(k) = \epsilon(-k)$ is preserved for very general energy dispersion laws. A superconducting ground state can thus be stabilized for $(TM)_2X$ compounds. The critical temperature never exceeds 2 K. High pressure is required for the superconductivity of sulfur compounds $(TMTTF)_2Br$ (Balicas et al., 1994), Fig. 10, and selenium compounds $(TMTSF)_2PF_6$ (Jérome et al., 1980), Fig. 11. $(TMTSF)_2ClO_4$ is the only member of the $(TM)_2X$ series in which superconductivity exists under ambient pressure (Bechgaard et al., 1981). What has emerged from the study of $(TM)_2X$ superconductors is the strong competition existing between superconducting and DW instabilities governed by the FS nesting. Attempts to raise T_c (superconductivity) in $TMTSF_2ReO_4$ using a pressure cycling procedure to prevent the formation of an anion ordered insulating phase has led to the stabilization of the more stable SDW phase (Tomič and Jérome, 1989). Therefore, T_c cannot be raised above 1.3 K but superconductivity in the $(TM)_2X$ series develops in a background of AF

spin fluctuations. Unlike 2D superconductors which are the subject of the next section, the properties of the anisotropic 1D superconducting state have not yet been studied in details.

3 Two dimensional conductors

3.1 Ground states

When 2D organic superconductors first appeared, they became very popular for a lot of reasons. Rather high superconducting T_c (as compared to the $(TM)_2X$ series) could be stabilized in the phase β_H-$(ET)_2I_3$ (T_c = 8 K) (Laukhin et al., 1985; Creuzet et al., 1985) and T_c = 9.4 K in κ-$(ET)_2Cu(NCS)_2$ (Urayama et al., 1988), Fig. 11, or even 11.4 and 12.8 K in κ-$(ET)_2Cu[N(CN)_2]Br$ (Kini, 1990) and κ-$(ET)_2Cu[N(CN)_2]Cl$ under 0.3 kbar (Williams et al., 1990) respectively. Owing to the very pronounced 2D character of the FS, textbook examples for quantum oscillations of the magnetization and resistivity have been observed in κ-$(ET)_2Cu(NCS)_2$ (Oshima et al., 1988) and β_H-$(ET)_2I_3$ (Kang et al., 1989) leading to a detailed determination of the FS (Wosnitza, 1995). The importance of magnetism in 2D conductors is less apparent than for Q-1D conductors since the absence at first sight of any nesting feature on the FS precludes the stabilization of SDW phases. Consequently, several 2D conductors remain metallic down to low temperatures. At variance with Q-1D conductors, what is exceptional for 2D conductors is the absence of magnetism under ambient pressure. There are, however, some indications that in these systems too, superconductivity is located close to an insulating state which shows magnetic properties. The relevance of magnetism becomes clear from the phase diagram in Fig. 12 displaying the different ground states which can be stabilized in the κ-$(ET)_2CuX$ series varying the nature of the anion CuX or the pressure parameter. The origin of pressure has been fixed at the compound κ-$(ET)_2Cu[N(CN)_2]Cl$ undergoing the onset of a magnetic modulation below 26 K (Miyagawa et al., 1995). The magnetic nature of the ground state is also supported by the observation of an antiferromagnetic resonance in ESR experiments. Furthermore, ^{13}C and ^{1}H-NMR data suggest the stabilization of a commensurate magnetic structure with an amplitude of 0.4–1 μ_B which is about ten times the amplitude measured in the $(TM)_2X$ series. The origin for such a commensurate magnetic ground state is not clear at the moment as the FS of these 2D conductors does not reveal any obvious commensurate nesting vectors. In spite of its unknown origin the interplay between magnetism and superconductivity is obvious in Fig. 12. A minute pressure of 0.3 kbar is enough to suppress the magnetic ground state and stabilize superconductivity below 12.8 K (Sushko et al., 1993).

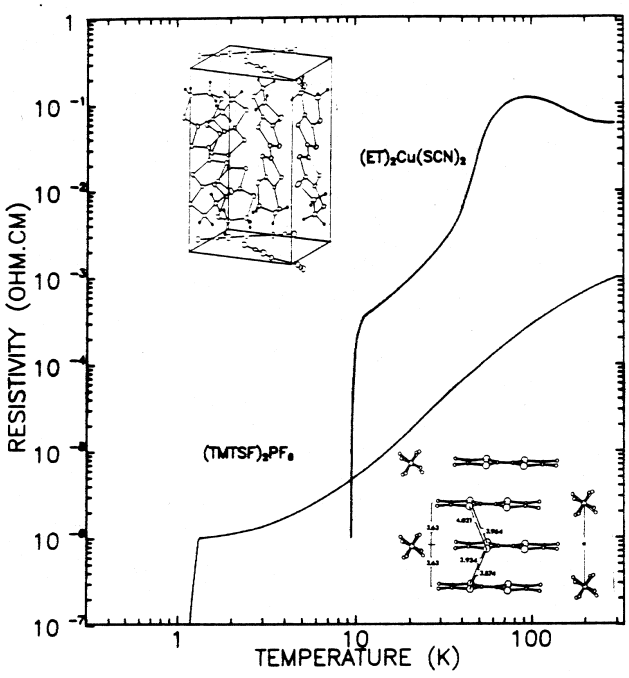

Figure 11. Superconductivity at 1 K in $(TMTSF)_2PF_6$ under 9 kbar and at 9 K in κ-$(ET)_2Cu(NCS)_2$ at ambient pressure.

3.2 Magnetic fluctuations at high temperature

Although the role of Coulomb repulsions in 2D conductors could be anticipated from the early data of frequency dependent optical conductivity leading to $U/W \approx 1$ (Jacobsen, 1987; Jérome, 1994). This is the NMR investigation of κ-phase conductors which confirm that magnetic fluctuations govern the electronic properties of the conducting phase at high temperature. First, the pressure dependence of the Knight shifts (KS) in κ-Br is large (-6% kbar^{-1}) and can only be explained if the on-site Coulomb repulsion to bandwidth ratio is of the order unity (Mayaffre et al., 1994). Secondly, an anomalous temperature dependence was found for the Knight shift and the spin-lattice relaxation rate (Mayaffre et al., 1994), Fig. 13. At ambient pressure, the Knight shift shows a smooth T-dependence between 300 and 50 K which can be understood by the thermal contraction but below 50 K a further pronounced drop of the susceptibility is observed (Kataev et al., 1992). Concomitantly, $(T_1T)^{-1}$ reveals near 50 K an important enhancement which obviously departs from the usual Korringa relation (Mayaffre et al., 1994; Kawamoto

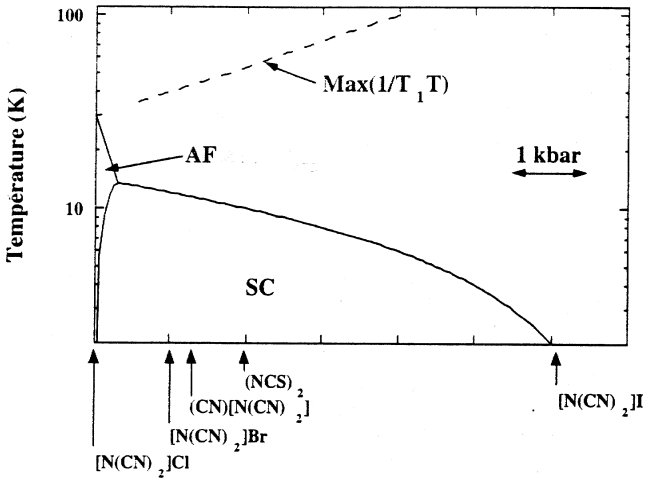

Figure 12. Generalized phase diagram for the κ-$(ET)_2CuX$ 2D conductors.

et al., 1995). This behaviour of the relaxation rate seems to be general for most κ-phase materials. At a pressure of 4 kbar, all anomalies of KS and $(T_1T)^{-1}$ are removed and a Korringa law is recovered (Mayaffre et al., 1994). The temperature profile of both $(T_1T)^{-1}$ and KS suggest the existence of a pseudo-gap in the density of states and of strong spin fluctuations at a wave vector nesting the 2D Fermi surface. Besides magnetic properties there exists an anomalous behaviour for the resistivity as well in the same temperature range. The temperature of 50 K is the temperature where a peak of dR/dT is observed (Sushko, 1991). As for $(T_1T)^{-1}$ or KS, a regular behaviour of the metallic conductivity is recovered under a pressure of ≈ 4 kbar (Sushko, 1991).

3.3 Comparison with high T_c cuprates

The temperature profiles of $(T_1T)^{-1}$ and KS show a striking similarity with those reported in underdoped cuprates, for example via ^{63}Cu-NMR in $YBa_2Cu_3O_{6.63}$ (Takigawa et al., 1991). This relaxation behaviour in HTSC has often been explained by the existence of short range AF correlations in the CuO_2 planes giving rise to a gap in the spin excitations (Kampf and Schrieffer, 1990). However, for κ-ET_2X materials, the tight correlation between the relaxation peak and the temperature dependence of the resistivity makes it difficult to consider a decoupling between the spin and charge degrees of freedom. The origin of enhanced relaxation and transport scattering rate could be due to some nesting properties of the

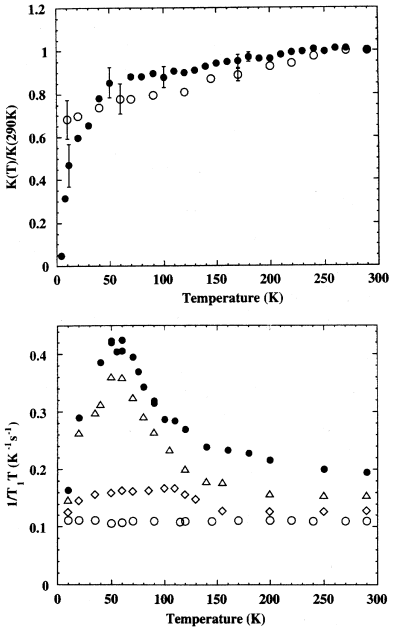

Figure 13. κ-$(ET)_2Cu[N(CN)_2]Br$ NMR under pressure. Temperature dependence of the Knight shift at 1 bar (•) and 4 kbar (○) normalized to the 300 K value (a) and of $(T_1T)^{-1}$ at different pressures 1, 1.5, 3 and 4 kbar from top to bottom (b).

2D Fermi surface with two possible incommensurate wave vectors connecting the flat portions (Oshima et al., 1988), Fig. 14. Both nuclear relaxation and electron scattering depend on the imaginary part of the spin susceptibility. Thus,

$$(T_1T)^{-1} \approx \sum_q \frac{\chi''(\mathbf{q},\omega_n)}{\omega_n} \tag{5}$$

If $\mathbf{Q}$ is the vector nesting the Fermi surface even partially, this features leads to an enhancement of the real part of the bare susceptibility $\chi_0'(\mathbf{q},\omega)$ at $\mathbf{q}=\mathbf{Q}$ and with the RPA $(T_1T)^{-1}$ reads (Charfi-Kaddour et al., 1992).

$$(T_1T)^{-1} \cong \sum_q \frac{1}{(1-U\chi_0'(\mathbf{q},\omega_n))^2} \frac{\chi_0''(\mathbf{q},\omega_n)}{\omega_n} \tag{6}$$

Therefore, a maximum of $(T_1T)^{-1}$ could derive from the nesting at the wave vector $\mathbf{Q}$ enhancing $\chi_0'(\mathbf{q},\omega_n)$ in Eq. (6). Going beyond the RPA, the Fermi liquid theory in the presence of nesting properties explains the development of the pseudo gap in

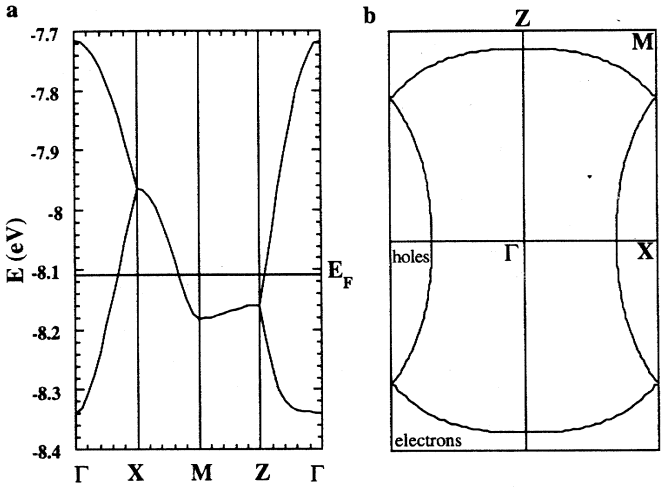

Figure 14. Calculated band structure (a) and Fermi surface (b) of κ-$(ET)_2Cu[N(CN)_2]Br$, after Canadell (1996).

the density of states at the Fermi level. Such pseudo-gap would affect the static and dynamic susceptibility explaining both the drop of KS and the peak of relaxation. Furthermore, the peak of resistivity can be attributed to the enhanced scattering against AF fluctuations. The high pressure work shown how the various manifestations of AF fluctuations on magnetism and transport vanish very quickly. T_1 or the pseudo gap, being related to the nesting properties are much more sensitive to pressure than the high temperature Knight shift (or susceptibility). Furthermore, as observed in Q-1D superconductors the suppression of AF fluctuations under pressure goes together with the disappearance of superconductivity. This observation emphasizes the experimental relation between spin fluctuations and superconductivity in both 1D and 2D series of organic superconductors (Wzietek et al., 1996).

4 Fullerides

4.1 Phase 3 fullerides

Among the various kinds of A_xC_{60} fullerides superconducting compounds A_3C_{60} (A = K, Rb, Cs) are probably those in which magnetism plays the smallest role. The metallic character of A_3C_{60} is fairly well understood in terms of a half filling of a band deriving from the six threefold-degenerate lowest unoccupied molecular

orbital (LUMO) of C_{60}. The study of the spin susceptibility of K_3C_{60} via ^{13}C Knight shift and T_1 measurements (Kerkoud et al., 1994) reveals a very small pressure coefficient ($\approx -1\%$ kbar^{-1}) which is in fair agreement with the pressure dependence of the band structure neglecting Coulomb interaction. In addition, the superconducting transition of phase 3 compounds with different alkali atoms or under pressure supports an interpretation in terms of a weak coupling BCS model with a pairing interaction mediated by intramolecular electron-phonon coupling (Haddon, 1992).

4.2 Phase 4 fullerides

In A_4C_{60} compounds, four levels among the six threefold-degenerate t_{1u} orbitals are occupied by alkali metals electrons implying a partial filling of the band in the solid. However, the metallic character which could be expected from the partial band filling is not observed from photoemission spectra (Benning et al., 1992) optical conductivity (Iwasa et al., 1993) and thin film resistivity (Haddon et al., 1994) data. Furthermore, ESR susceptibility (Kosaka et al., 1993) and T_1^{-1} data (Zimmer et al., 1994) show the non-magnetic and insulating nature of the ground state, Fig. 15. However the nuclear spin-lattice relaxation is very fast at room temperature and cannot be explained by a straightforward semiconducting band structure model. Following an NMR investigation under pressure (Kerkoud et al., 1996), an interplay between the molecular Jahn-Teller and the energy dispersion has been proposed for the interpretation of the electronic properties of A_4C_{60}. The t_{1u} manifold is split into three components with two lower degenerate components filled by the four alkali atom electrons and one empty higher component. Moreover, the molecular interaction gives rise to the broadening of the molecular level into a semiconducting band scheme. If the Jahn-Teller effect Δ_{JT} is strong enough to overcome the band broadening an insulating material is obtained. The fast relaxation at room temperature has been explained by intrinsic localized paramagnetic centers provided by local excitations of the C_{60}^{4-} molecules. The lowest excited state $(C_{60}^{4-})^*$ differs from C_{60}^{4-} by the inverse arrangement of the doubly degenerate and non degenerate Jahn-Teller levels. The lower level is completely filled by two electrons and the higher is half-filled by the two residual electrons. The latter, according to the Hund's rule form a triplet state giving rise to thermally activated localized paramagnetic centers with an activation energy which amounts to $\Delta_{JT}/2$. A Jahn-Teller splitting of 140 meV has been derived from the activated temperature dependence of T_1^{-1} in Rb_{60}^{4-}. The exciton level at $\Delta_{JT}/2$ lies within the Jahn-Teller gap and at increasing pressure the bandwidth increases with a concomitant merging of the localized states into the itinerant states. The material evolves from a narrow gap semiconductor with localized paramagnetic excitations

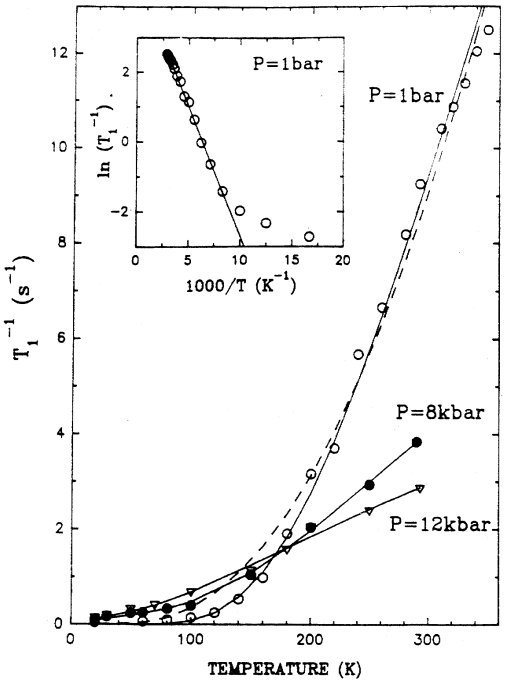

Figure 15. Temperature dependence of ^{13}C-T_1^{-1} in Rb_4C_{60} for different pressures. The fit with the model of localized triplet excitons (Kerkoud et al., 1996) is shown by the continuous line at 1 bar. The relaxation of thermally activated carriers in a semiconductor would follow the dashed line.

at ambient pressure to a semimetal under a pressure of 12 kbar as shown from the recovery of the Korringa behaviour for T_1^{-1}, Fig. 15.

4.3 Phase 1 fullerides

A_1C_{60} forms a remarkable system where the stabilization of an itinerant magnetic ground state has been identified for the first time in the A_xC_{60} series (Chauvet et al., 1994). A_1C_{60} undergoes a first-order structural transition around 350 K between a fcc phase at high temperature and an orthorhombic phase at low temperature (Stephens et al., 1994). The orthorhombic phase is particular as it exhibits a polymerized structure along chains of C_{60} molecules. ESR (Pekker, 1994) and optical conductivity (Bommelli et al., 1995) data support the conducting nature of A_1C_{60} down to 50 K. However, the progressive opening of a pseudo-gap in $N(E_F)$ is observed at low temperatures (Chauvet et al., 1994) and a magnetic ground state

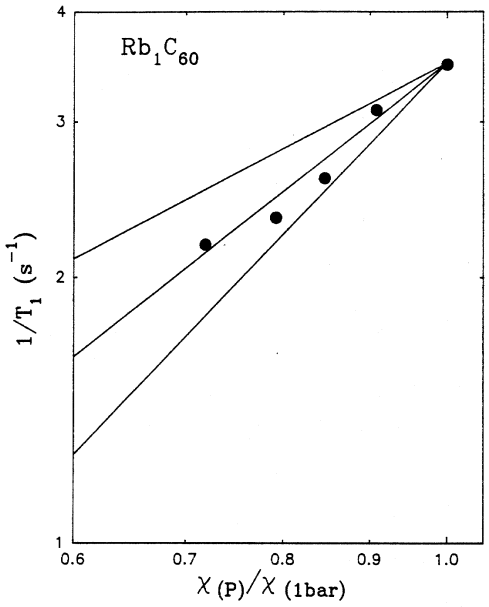

Figure 16. Relation between ^{13}C-T_1^{-1} and χ_S in Rb_1C_{60} when the pressure is varied between 1 bar and 4.5 kbar. The best fit is obtained for $T_1^{-1} \approx \chi^{3/2}$.

sets in below 20 K (Uemura et al., 1995; Mac Farlane et al., 1995). The unusually large pressure coefficient of the susceptibility ($\approx -9\%$ kbar^{-1}) (Forro et al., 1996) reveals the importance of the exchange enhancement in these materials with a Stoner factor of about 3 under ambient conditions (Auban-Senzier et al., 1996). The magnitude of the enhancement may be explained by two specific features for phase 1 fullerides. First, the calculation of the effective Coulomb repulsion taking into account the Jahn-Teller energy and the bare on-site repulsion provides a value of 0.2 eV for Rb_1C_{60} but nearly negligible for A_3C_{60} (Victoroff et al., 1995). Secondly, a large contribution to $N(E_F)$ can be expected from a singularity in the density of states located in the vicinity of the Fermi energy (Victoroff and Héritier, 1996).

The nature of magnetic fluctuations is still very controversial. One-dimensional AF fluctuations, related to the polymerized structure have been claimed to persist up to room temperature on the basis of a temperature independent nuclear relaxation (Brouet et al., 1996). However, this suggestion is in agreement neither with the conducting character of the compound nor with the experimental relation between T_1 and χ_S leading to $1/T_1 \approx \chi_S^{3/2}$ or χ_S^2 which is followed (Moriya, 1995),

Fig. 16, as the pressure is increased up to 6 kbar (Auban-Senzier et al., 1996). What has been proposed instead is the model of ferromagnetic fluctuations within chains or planes of the body centered orthorhombic structure of A_1C_{60}. AF-fluctuations between planes grow below 50 K and provide a two-sublattice magnetic ground state at 15-20 K (Erwin et al., 1995). The band structure calculation (Erwin et al., 1995) has shown that the 3D AF-modulation opens a gap at the Fermi level and makes the ground state insulating. The magnetic ground state is suppressed under pressure as shown by NMR data under pressure, Fig. 17, but at 6 kbar even in the absence of long range ordered magnetism strong 3D AF-fluctuations remain, in the incipient antiferromagnet as indicated by the temperature dependence of the relaxation,$1/T_1 \approx T^{1/4}$ (Moriya, 1995). Under 12 kbar, the existence of a Korringa relaxation down to the lowest temperatures supports the existence of a weakly correlated metallic phase bearing much resemblance with the conducting phases of Rb_3C_{60} at ambient pressure or Rb_4C_{60} under pressure.

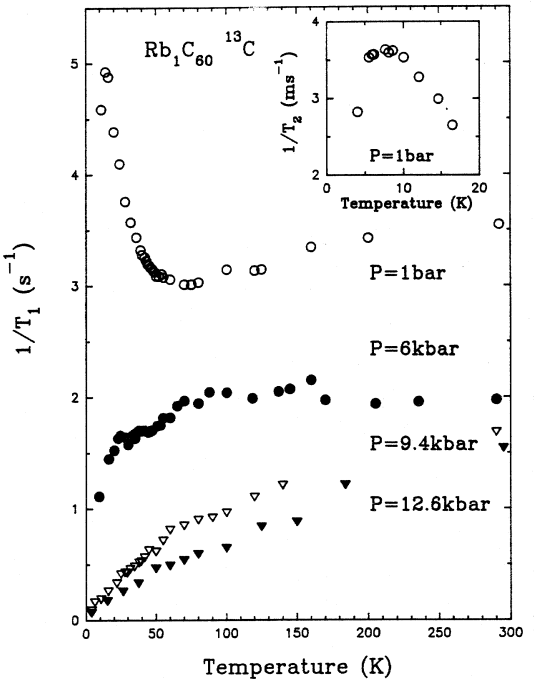

Figure 17. Temperature dependence of ^{13}C-T_1^{-1} at different pressures.

5 Conclusion

Organic superconductivity has been around for the last 15 years. Remarkable progresses have been achieved in terms of increasing the stability of the superconducting state from 1K in one dimensional organic conductors pertaining to the $(TM)_2X$ series up to 30 K in the fullerides. The systematic study of isostructural series of either 1D or 2D conductors has shown that the phase diagrams exhibit magnetic phases in close proximity to the superconducting state. Furthermore, superconductivity emerges out of a "normal conducting" state in which the presence of magnetic fluctuations has been clearly identified by a wealth of NMR data. As far as 1D conductors are concerned, the U/W ratio is close to unity and the interplay between the half-filling character (the Umklapp scattering term) and the interchain overlap (the cross-over temperature T_x) makes the generalized phase diagram remarkably diversified with spin-Peierls, SDW and superconducting ground states. Proximity between superconductivity and magnetism is also observed in high T_c superconductors with a noticeable difference since the critical temperature reaches zero at the borderline. The anisotropic character of the pairing interaction in 2D organics is inferred from the gapless character of the quasi particle energy spectrum. However, the symmetry of the order parameter is still waiting for phase-sensitive experiments. In this context the role of magnetic fluctuations in pair formation of organic superconductors has to be clarified (Mayaffre et al., 1995). In spite of the narrow bandwidth, magnetism is less present in the series of A_xC_{60} fullerides. Only in A_1C_{60} uniform spin fluctuations are observed at high temperature and the AF coupling between ferromagnetic planes allows the stabilization of an AF ground state at low temperature. High pressure decreases the importance of magnetic fluctuation and suppresses the stability of the AF ground state.

Acknowledgements

This article is based to a large extent on the results of the research performed at Orsay over the last decade. I gratefully acknowledge the constant cooperation of my colleagues in our laboratory and C. Bourbonnais at Sherbrooke. This publication in the Journal of the Royal Danish Academy of Sciences and Letters is a great opportunity to acknowledge the very fruitful cooperation between K. Bechgaard and his group at Copenhagen and the University Paris-Sud which has been successfully running over the past 20 years. No doubts, this active cooperation has been decisive for the development of organic conductors.

References

Auban P et al., 1989: J. Phys. (Paris) **50**, 2727
Auban-Senzier P et al., 1996: J. Phys. (Paris) I, in press
Balicas L et al. 1994: J. Phys. (Paris) I, **4**, 1539
Barisič S and Brazovskii S, 1979: in *Recent Development in Condensed Matter Physics*, ed. JT Devreese (Plenum Press, New York) p. 327
Barthel E et al., 1993a: Europhys. Lett. **21**, 87
Barthel E, Kriza G, Quirion G, Wzietek P, Jérome D, Christensen JB, Jørgensen M and Bechgaard K, 1993b: Phys. Rev. lett. **71**, 2825
Barthel E, 1994: Thesis (Université Paris-Sud, Orsay)
Bechgaard K et al., 1980: Solid State Commun. **33**, 1119
Bechgaard K et al., 1981: Phys. Rev. Lett. **46**, 852
Benning PJ et al., 1992: Phys. Rev. B **45**, 6899
Bommeli F et al., 1995: Phys. Rev. B **51**, 14794
Bourbonnais C and Caron L, 1986: Physica B **143**, 451
Bourbonnais C, 1987: in *Low dimensional Conductors and Superconductors*, eds. D. Jérome and LG Caron (Plenum Press, New York) p. 155
Brouet V et al., 1996: Phys. Rev. Lett. **76**, 3638
Brown S et al., 1997: to be published
Canadell E, 1995, private communication
Canadell E, 1996, private communication
Charfi-Kaddour S et al., 1992: J. Phys. I **2**, 1853
Chauvet O et al., 1994: Phys. Rev. Lett. **72**, 2721
Clark WG, 1996: private communication
Creuzet F et al., 1985: J. Phys. Lett. (Paris) **46**, L-1079
Ducasse L et al. 1986: J. Phys. C **19**, 3805
Emery V et al., 1982: Phys. Rev. Lett. **48**, 1039
Emery V, 1983: J. Phys. (Paris) Coloq. **44** C3-977
Erwin SC et al., 1995: Phys. Rev. B **51**, 7345
Forro L. et al., 1996: Proceedings of the Kirchberg Conference
Goze C, 1996: Thesis (Univ. Montpellier)
Grüner G, 1988: Rev. Mod. Phys. **60**, 1129
Grüner G, 1994: Rev. Mod. Phys. **66**, 1
Haddon R 1992: Acc. Chem. Res. **25**, 127
Haddon R et al., 1994: Chem. Phys. Lett. **218**, 100
Hebbard A.F. et al., 1985: Nature **350**, 600
Ishiguro T and Yamaji K, 1990: *Organic Superconductors*, (Springer-Verlag, Berlin) Vol. 88
Iwasa Y et al., 1993: J. Phys. Chem. Solids **54**, 1795
Jacobsen CS, 1987: in *Low Dimensional Conductors and Superconductors*, eds. D. Jérome and L. Caron (Plenum Press, New York)
Jérome D, 1994: in *Organic Conductors*,ed. J.P. Farges (Dekker, New York) p. 405,
Jérome D and Schulz HJ, 1982: Adv. Phys. **31**, 299
Jérome D et al., 1980: J. Phys. Lett. (Paris) **41**, L-95
Jérome D, 1991: Science **252**, 1509
Kampf A and Schrieffer R, 1990: Phys. Rev. B **41**, 6399
Kang W et al., 1989: Phys. Rev. Lett. **62**, 2559
Kataev V et al., 1992: Solid State Commun. **83**, 435
Kawamoto A et al., 1995: Phys. Rev. Lett. **74**, 3455
Kerkoud R et al., 1994: Europhys. Lett. **25**, 379

Kerkoud R et al., 1996: J. Phys. Chem. Solids **57**, 143
Kini AM et al., 1990: Solid State Commun. **69**, 503
Klemme BJ et al., 1995: Phys. Rev. Lett. **75**, 2408
Klemme BJ et al., 1996: J. Phys. (Paris) I, **6**, 1745
Kosaka M et al., 1993: Chem. Phys. Lett. **203**, 429
Kriza G et al., 1991: Phys. Rev. Lett. **66**, 1922
Kroto HW et al. 1985: Nature **318**, 162
Laukhin VN et al. 1985: Sov. Phys. JETP Lett. **41**, 81
Mac Farlane WA et al., 1995: Phys. Rev. B **52**, R 6995
Mayaffre H et al., 1994: Europhys. Lett. **28**, 205
Mayaffre H et al., 1995: Phys. Rev. Lett. **75**, 4122
Miyagawa K et al., 1995: Phys. Rev. lett. **75**, 1174
Moriya T, 1963: J. Phys. Soc. Jpn. **18**, 516
Moriya T, 1995: in *Spectroscopy of Mott insulators and Correlated Metals*, eds. A. Fujimori and Y. Tokura (Springer-Verlag, Berlin) p. 66
Oshima K et al., 1988: Phys. Rev. B **38**, 938
Pekker S 1994: Solid State Commun. **90**, 349
Pouget JP et al., 1982: Mol. Cryst. Liq. Cryst. **79**, 129
Pouget JP, 1996: J. Phys. (Paris) I, **6**, 1501
Schulz HJ, 1991: Int. J. Mod. Phys. B **5**, 57
Solyom J, 1979: Adv. Phys. **28**, 201
Stephens PW et al., 1994: Nature **370**, 636
Sushko YV et al., 1991: J. Phys. (Paris) I **1**, 1375
Sushko YV et al., 1993: Solid State Commun. **87**, 997
Takigawa M et al., 1991: Phys. Rev. B **43**, 247
Tomič S and Jérome D, 1989: J. Phys. Condens. Matter **1**, 4451
Traetteberg O et al., 1994: Phys. Rev. B **49**, 409
Uemura YJ et al., 1995: Phys. Rev. B **52**, R 6991
Urayama H, et al., 1988: Chem. Lett. **55**, 1988
Victoroff W and Héritier M, 1996: J. Phys. (Paris) I, **6**, 2175
Victoroff W et al., 1995: Synthetic. Metals **71**, 1489
Williams JM et al., 1991: Science **252**, 1501
Williams JM et al. 1990: Inorg. Chem. **29**, 3272
Wosnitza J, 1995: in Springer Series in Solid State Science (Springer-Verlag, Berlin)
Wzietek P, 1993: J. Phys. (Paris) I **3**, 171
Wzietek P et al., 1996: J. Phys. (Paris) I, **6**,2011
Zimmer G et al., 1994: Europhys. Lett. **27**, 543